Rectification of the Bias in the Wavelet Power Spectrum

YONGGANG LIU

College of Marine Science, University of South Florida, Saint Petersburg, Florida, and School of Oceanography, University of Washington, Seattle, Washington

X. SAN LIANG

Courant Institute of Mathematical Sciences, New York University, New York, New York

ROBERT H. WEISBERG

College of Marine Science, University of South Florida, Saint Petersburg, Florida

(Manuscript received 7 July 2006, in final form 31 October 2006)

ABSTRACT

This paper addresses a bias problem in the estimate of wavelet power spectra for atmospheric and oceanic datasets. For a time series comprised of sine waves with the same amplitude at different frequencies the conventionally adopted wavelet method does not produce a spectrum with identical peaks, in contrast to a Fourier analysis. The wavelet power spectrum in this definition, that is, the transform coefficient squared (to within a constant factor), is equivalent to the integration of energy (in physical space) over the influence period (time scale) the series spans. Thus, a physically consistent definition of energy for the wavelet power spectrum should be the transform coefficient squared divided by the scale it associates. Such adjusted wavelet power spectrum results in a substantial improvement in the spectral estimate, allowing for a comparison of the spectral peaks across scales. The improvement is validated with an artificial time series and a real coastal sea level record. Also examined is the previous example of the wavelet analysis of the Niño-3 SST data.

1. Introduction

Wavelet analysis may be advantageous over the classical Fourier analysis in that it unfolds a time series not only in frequency but also in time, which is especially useful when the signal is nonstationary. Because of this property, wavelet analysis has been widely applied across disciplines since its introduction in the early 1980s. See Daubechies (1992), Chui (1992), Meyer (1992), Strang and Nguyen (1997), Percival and Walden (2000), and references therein, for a historical account. Applications in atmospheric and oceanic sciences have also been documented for over a decade (e.g., Gamage and Blumen 1993; Liu 1994; Gu and Philander 1995; Willemsen 1995; Liu and Miller 1996; Wang and Wang 1996; Percival and Mofjeld 1997; Haus et al. 1999; Haus and Graber 2000); several useful reviews on this topic can be found in Meyers et al. (1993), Lau and Weng (1995), Torrence and Compo (1998, hereafter TC98), Domingues et al. (2005), and Labat (2005), to name a few. Among these, TC98 is probably the most celebrated one, with over 800 citations so far. A practical step-by-step guide is given, and software packages in FORTRAN, IDL, and MATLAB languages are provided for free download from their Web site (http://atoc.colorado.edu/research/wavelets/).

It has been observed in the atmosphere–ocean community that wavelet power spectra are distorted or biased in favor of large scales or low frequencies [see the frequently asked questions (FAQs) on Torrence and Compo's above-mentioned Web site and also the documents of the associated software]. That is to say, for a time series comprising two sine waves of the same amplitude but distinct frequencies, a wavelet analysis will yield two spectral peaks of different magnitude, the one on the low frequency being larger. This counters our expectation and is also in contrast to the result of any classical global analysis such as Fourier transform, making comparison of the peaks across the scales impossible. For this reason, it is suggested that if sharp peaks

Corresponding author address: Yonggang Liu, School of Oceanography, University of Washington, Box 355351, Seattle, WA 98195.
E-mail: yliu18@gmail.com

DOI: 10.1175/2007JTECHO511.1

are found in a power spectrum, then certain types of wavelet spectra should not be used to determine their relative magnitudes (see the above-mentioned online FAQs). This issue may greatly limit the usage of wavelet analysis in solving real atmosphere–ocean problems, as sharp peaks are more often than not identified.

On the other hand, the equivalence in different scale reconstructions has been rigorously established between the orthonormal localized transforms such as wavelet transform and the global analyses such as the average-departure decomposition for stationary time series (cf. Liang and Anderson 2007, hereafter LA06). This implies that the spectra resulting from the global and the local analyses should be consistent. In other words, there should not be such spectral "bias." The wavelet spectral estimates in the mainstream of the community need improvements. [Some wavelet applications do not have this bias problem, e.g., Liang and Robinson (2004).] The purpose of this paper is to address this bias problem.

The rest of this paper is arranged as follows. The bias problem is further illustrated with a real ocean time series in section 2. In section 3, theoretical derivations are followed to shed light on what is underlying a power spectral analysis. A physically consistent definition of energy, and hence an alternate formalism of power spectrum, are proposed, which allows for a solution of the problem. The improvement of the biased spectrum by the new formalism is validated in sections 4, 5, and 6, respectively, with idealized and real world examples. A summary and discussion are then provided in section 7.

2. The raising of the issue

a. Data and data processing

Time series of hourly coastal sea level at St. Petersburg, Florida, are from the National Oceanic and Atmospheric Administration/National Ocean Service (NOAA/NOS) (http://www.co-ops.nos.noaa.gov) from January 1993 through December 2005. After quality control, the sea level record is de-tided by removing the four major tidal constituents: *M2*, *S2*, *K1*, and *O1*, using the T_Tide Harmonic Analysis Toolbox of Pawlowicz et al. (2002). It is then 48-h low-pass filtered, 12-h subsampled, and adjusted for the inverse barometer effect. Now the time series contains mainly subtidal sea level variations (Fig. 1, top). The air pressure data are from two NOAA/National Data Buoy Center (NDBC) stations, 42036 and VENF1 (Venice, Florida) (http://www.ndbc.noaa.gov/), and from University of South Florida surface buoys on the West Florida Shelf. The locations of the sea level and meteorological stations can be found in Fig. 1 of Liu and Weisberg (2005a).

b. The wavelet power spectrum based on TC98

The MATLAB wavelet package of TC98 is used to analyze the subtidal sea level time series. Following the guide of TC98, the wavelet parameters are chosen as follows. The wavelet base function is chosen to be Morlet, which is often used in analyzing geophysical data. A start scale of 2 days is specified since this is the smallest actual time scale for the 48-h low-pass-filtered time series. The spacing between the discrete scales, dj, is chosen as 1/8; that is, there are 8 suboctaves per octave. The total number of scales is determined by both dj and j_1, where j_1 is the number of the octaves; here it is set to be 9. Thus, there are $dj \times j_1 + 1 = 73$ scales ranging from 2 to 1024 days. The wavelet transform is converted to wavelet power spectrum as instructed in the sample MATLAB program.

The wavelet power spectrum of the subtidal St. Petersburg sea level is shown in the middle panel of Fig. 1. To our surprise, the spectrum is seriously biased in the frequency domain, so that the annual time scales outperform the synoptic weather time scales so much that the latter seems negligible in the wavelet power spectrum. This is unacceptable for the subtidal sea level fluctuations on the West Florida Shelf (WFS), where the synoptic winds play a dominant role on the inner WFS circulation and hence affect the coastal sea level fluctuation on synoptic time scales (e.g., Marmorino 1982; Mitchum and Sturges 1982; Cragg et al. 1983; Li and Weisberg 1999; He et al. 2004; Liu and Weisberg 2005a,b, 2007; Liu et al. 2007; Weisberg et al. 2005). Thus, the usefulness of the wavelet analysis seems to be doubtful for the subtidal sea level data.

Statistical significance testing is also provided in TC98. In the middle panel of Fig. 1, the black contour encloses regions of greater than 90% confidence for a red-noise process with a lag-1 coefficient of 0.9. It can be seen that these regions include both the synoptic and annual time scales; that is, the wavelet spectra are statistically significant on these two time scales. The biased wavelet spectrum needs improvement, at least visually, to be consistent with the statistical significance test.

3. Energy and physically consistent wavelet power spectrum

To resolve the problem, we need to go back to the definition of energy in functional analysis. A rigorous treatment and detailed interpretation in the context of atmospheres and oceans is referred to by Liang and Robinson (2005). Some of the facts pertaining to wavelet transform are briefly presented in this section.

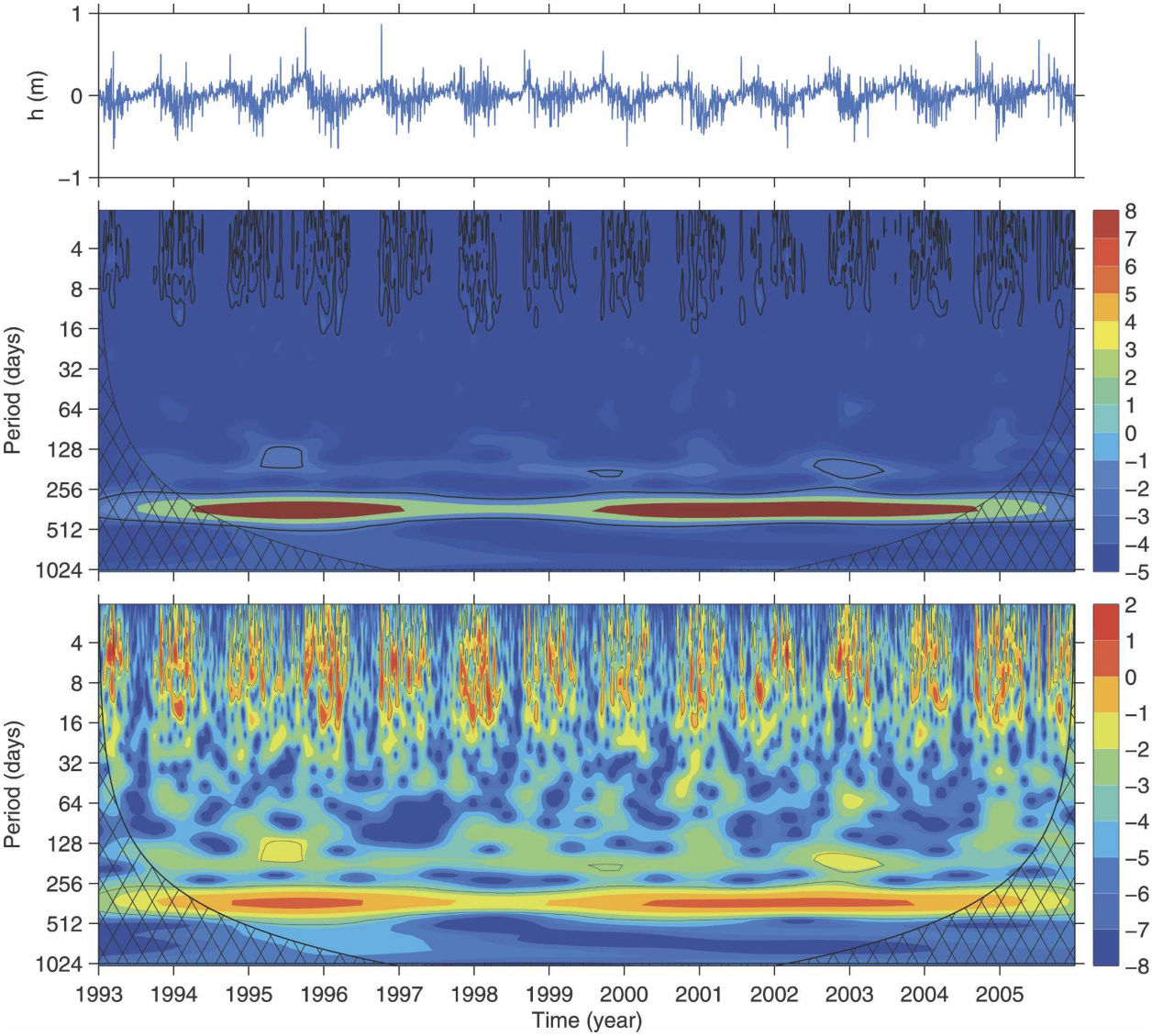

FIG. 1. (top) The time series of St. Petersburg sea level after 48-h low-pass filtering and 12-h subsampling. Also shown are the (middle) original and (bottom) rectified wavelet power spectra in logarithm (base 2). The regions of greater than 90% confidence are shown with black contours. Cross-hatched regions on either end indicate the "cone of influence," where edge effects become important.

Suppose we have a time series $f(t)$, where t is defined on some finite interval that may be assumed to be [0, 1] without loss of generality. If t is not in this range, a rescaling can always make it so. Suppose the wavelet basis is

$$\psi_n^j(t) = 2^{-j/2}\psi(2^j t - n), \tag{1}$$

where t is on the real line $\Re$, integers j and n are the scale level (2^{-j} the scale) and the time location, respectively; and ψ is the mother wavelet that forms an orthonormal set with respect to j and n in the function space[1] over $\Re$. The finite interval must be extended to the whole real line before an analysis can be performed. Commonly used extension schemes include zero padding, periodization, and extension by reflection (cf. Strang and Nguyen 1997); for example, zero padding is used in TC98. It has been proved that a scheme of these essentially introduces another basis for the function space over [0, 1], which also forms an orthonormal set

[1] We always study the problems in some L_2 space, that is, a space containing square integrable functions over the definition domain.

therein (LA07).[2] It suffices to write the new basis symbolically as $\tilde{\psi}^j_n(t)$, $t \in [0, 1]$. Detailed expression can be found in LA07 (their section 2.3) or, when only periodization is used, in Meyer (1992). Here $\tilde{\psi}^j_n$ is a "modified wavelet basis" from ψ^j_n. The wavelet transform now can be identically expressed with $\tilde{\psi}^j_n$ over [0, 1]. The transform–reconstruction pair of f is thereby

$$\hat{f}^j_n = \int_0^1 f(t)\tilde{\psi}^j_n(t)\,dt, j \geq 0, n = 0, 1, \ldots, 2^j - 1, \quad (2)$$

$$f(t) = f_0 + \sum_{j=0}^{\infty}\sum_{n=0}^{2^j-1} \hat{f}^j_n\tilde{\psi}^j_n(t), \quad (3)$$

where f_0 is a part related to scales larger than the time span, on which we do not intend to elaborate; in the case of extension by periodization, this part is simply the mean over [0, 1], as proved by LA07 (theorem 4.2). Notice the range in which n runs; it is a finite set and scale dependent. On a specific scale level j, the reconstruction, that is, the projection of f onto the subspace containing only features of scale 2^{-j}, is

$$f^j(t) = \sum_{n=0}^{2^j-1} \hat{f}^j_n\tilde{\psi}^j_n(t), t \in [0, 1], j > 0. \quad (4)$$

We do not consider scale level $j = 0$ here, as it contains an extra term that is not helpful to our illustrative purpose. In Eq. (4), the $f^j(t)$ is a (1D) field variable. The energy on scale level j at time t is then simply $[f^j(t)]^2$, up to some constant factor as needed. How is the energy represented by the transform coefficients $\hat{f}^j_n$?

A theorem connecting the phase space representation and the physical space field quantity answers the question. This is the generalized Parseval relation. In an L_2 space, as considered here, it reads, if the transform is orthonormal,[3]

$$\int_0^1 [f^j(t)]^2\,dt = \sum_{n=0}^{2^j-1} [\hat{f}^j_n]^2. \quad (5)$$

The lhs is the energy in the physical sense, followed by an integration with respect to t over its definition domain; the rhs is the summation of $N = 2^j$ parts, each part representing the process on a small interval D_n centered around $t = 2^{-j}n$, with a length of $\Delta t = 1/N = 2^{-j}$. We may replace the lhs integration by a Riemann sum of N parts, according to the middle value theorem of integral,

$$\int_0^1 [f^j(t)]^2\,dt = \sum_{n=0}^{2^j-1} [f^j(t_n)]^2\Delta t_n, \quad (6)$$

where $\Delta t_n = \Delta t$, and t_n lies somewhere on the small interval D_n. Here $f^j(t_n)$ is a field variable at time location t_n, and $[f^j(t_n)]^2$ is the energy in the physical sense (to within some constant factor), denoted by E^j_n. Comparing (5) and (6), we have

$$\sum_{n=0}^{2^j-1} E^j_n\Delta t_n = \sum_{n=0}^{2^j-1} [\hat{f}^j_n]^2. \quad (7)$$

So, a physically consistent definition of energy at location n (corresponding to $t = 2^{-j}n$) and scale level j (corresponding to scale 2^{-j}) in terms of the wavelet transform coefficients should be

$$E^j_n \equiv \frac{1}{\Delta t}[\hat{f}^j_n]^2 = 2^j \times [\hat{f}^j_n]^2. \quad (8)$$

We now can see why the wavelet spectral analysis widely adopted in the community (such as that in TC98) produces "biased" power spectra. The energy as conventionally defined is simply the square of $\hat{f}^j_n$, lacking the factor 2^j, the inverse of the scale. For two modes with identical amplitudes but different frequencies/scales, the power unfolded on the conventional wavelet spectrum appears different: The higher the scale level (smaller scale), the smaller the "energy"; that is, the high-frequency peaks tend to be underestimated. This is exactly what is often observed in the real application exercises, as documented by Torrence and Compo in the previously mentioned FAQ section of their Web site.

Lying at the heart of the conventional energy definition is the confusion between the energy and the integration of energy with respect to time: $\hat{f}^j_n$ is not a quantity just for the instant $2^{-j}n$ but a "bulk" variable containing information all over the neighborhood. Actually, the classical power spectral analyses also have the same problem; that is, we should multiply the square of the transform coefficients by some factor (inverse of the time span) to define the physically consistent energy. However, in a global analysis such as Fourier transform the factor is independent of scale, so the problem is disguised and is not an issue. In contrast, for localized analyses built on the basis of multiresolution analysis (Meyer 1992) such as wavelet transform, this

[2] What LA07 proved is with respect to a scaling function ϕ, or "father wavelet" (e.g., Meyer 1992). By multiresolution analysis, the subspace generated by $\{\psi^j_n\}_n$ is an orthogonal complement to that by $\{\phi^j_n\}_n$ in the space generated by the scaling basis at a higher level, $\{\phi^{j+1}_n\}_n$; the corollary with respect to wavelet functions thus follows immediately.

[3] This is not precisely true when an extension by reflection is used. But a similar theorem, called property of marginalization, applies. See LA07 (theorem 4.3).

issue surfaces. In an energetics analysis with a localized transform developed by themselves, Liang and Robinson (2005, pp. 203 and 222) emphasized the importance of the factor in physical process studies several times.

The above derivations rely on the orthonormality of the wavelet basis. We know that many popular wavelet transforms are not orthonormal or are with redundant sets called "frames" (e.g., Strang and Nguyen 1997). Strictly speaking, no notion of energy can even be introduced in a functional analysis if the basis is not orthonormal, as the energy thus defined is not conserved [Liang and Robinson 2005, LA07, their section 5, particularly Eq. (5.2)]. But in a loose sense, we may just use the above notion in the power spectrum calculation, that is, multiplying the conventionally produced spectra by 2^j (or dividing by the corresponding scale) to ensure physical consistency.

A final remark is on basis orthonormality. As mentioned above, rigorously there is no notion of energy in the sense of physics with nonorthonormal transforms. Although such wavelet transforms prove to be very useful in areas such as data compression and pattern identification, caution should be exercised when applying the results to real physical processes. For the same reason, spectra with different nonorthornormal bases may display the same pattern differently, because the process thus represented is not unique. In a field like atmosphere–ocean science, orthonormal analyses may need to be favored over nonorthonormal ones. Fortunately, it is easy to orthonormalize a basis if it possesses certain properties, as elucidated in Strang and Nguyen (1997). An organized treatment of orthonormalization can also be found in LA07 (their section 7.2).

4. The example problem revisited

The wavelet analysis of the St. Petersburg sea level time series is revisited. The power at each point in the spectrum is divided by the corresponding scale, based on the energy definition (8). The result is very encouraging (Fig. 1, bottom). The spectrum values over the synoptic time scales are enlarged and are now comparable to those on the annual time scales; it is also more consistent with the 90% significance level (the black contours in Fig. 1, middle and bottom). This makes more sense in light of coastal oceanography. Over the synoptic weather band the inner WFS ocean circulation is mainly driven by the local winds (e.g., Liu and Weisberg 2005a,b). The synoptic weather winds are seasonally modulated, stronger in winter but weaker in summer half years. These are displayed in the wavelet spectrum as a seasonal modulation of synoptic weather band sea level variation: The synoptic weather band energy is higher and more significant in winter than in summer half years. We also noticed that the wavelet energy on the annual time scales is lower in 1998. This corresponds to an anomalous event of WFS circulation conditions, indicative of a large interannual variation due to the impact of the Loop Current near Dry Tortugas (Weisberg and He 2003; Weisberg et al. 2005). In a word, the rectified wavelet spectrum estimates are now consistent with the physics of the coastal sea level variability on the WFS.

5. Test with sine waves

The above formalism of wavelet power spectrum is further tested with an artificial time series composed of sine waves of known frequencies and amplitudes. Five sine waves, with a unit amplitude and periods of 1, 8, 32, 128, and 365 days, respectively, are summed to form an artificial time series as shown in Fig. 2 (top). The sample interval is 1 h, and the length of the time series is 13 yr; both are comparable with those of the St. Petersburg sea level time series. The TC98 MATLAB program is used again, and the wavelet parameters are chosen as those for the sea level analysis with the following exceptions: the start scale is 6 h, and j_1 is set to be 12 so that the scale ranges from 6 h to 1024 days, covering the intrinsic periods of the sine waves.

The original localized wavelet power spectrum and the time-averaged wavelet spectrum (called "global wavelet spectrum" in TC98) are shown in the middle panel of Fig. 2. As expected, the spectral peaks are distorted, with the high-frequency peaks lower than the low-frequency peaks. However, when the spectrum is divided by the scale s, those spectral peaks have about the same height (Fig. 2, bottom), and the biased wavelet spectrum is rectified.

Both the original and rectified wavelet power spectra are shown again against the Fourier power spectrum in Fig. 3. The five Fourier spectral peaks have the same height (Fig. 3c), which is normal as expected from autospectral analysis. The improvement of the biased wavelet spectral peaks is substantial, as seen from their actual values (Figs. 3a,b). The bias seems much reduced when the spectrum is shown in logarithm (Figs. 3d,e). Maybe this partly explains why most wavelet users choose to show their wavelet spectra in logarithm. In Fig. 3b, the two spectral peaks at the low-frequency part (periods of 128 and 365 days) are a little smaller than the other three peaks (periods of 1, 8, and 32 days), which is due to the lower spectral values in the "cone of influence" (in Fig. 2, bottom) that resulted from zero padding (see the detailed explanation in TC98). Recall that the wavelet power spectrum in Fig. 3b is obtained by averaging the wavelet spectrum in

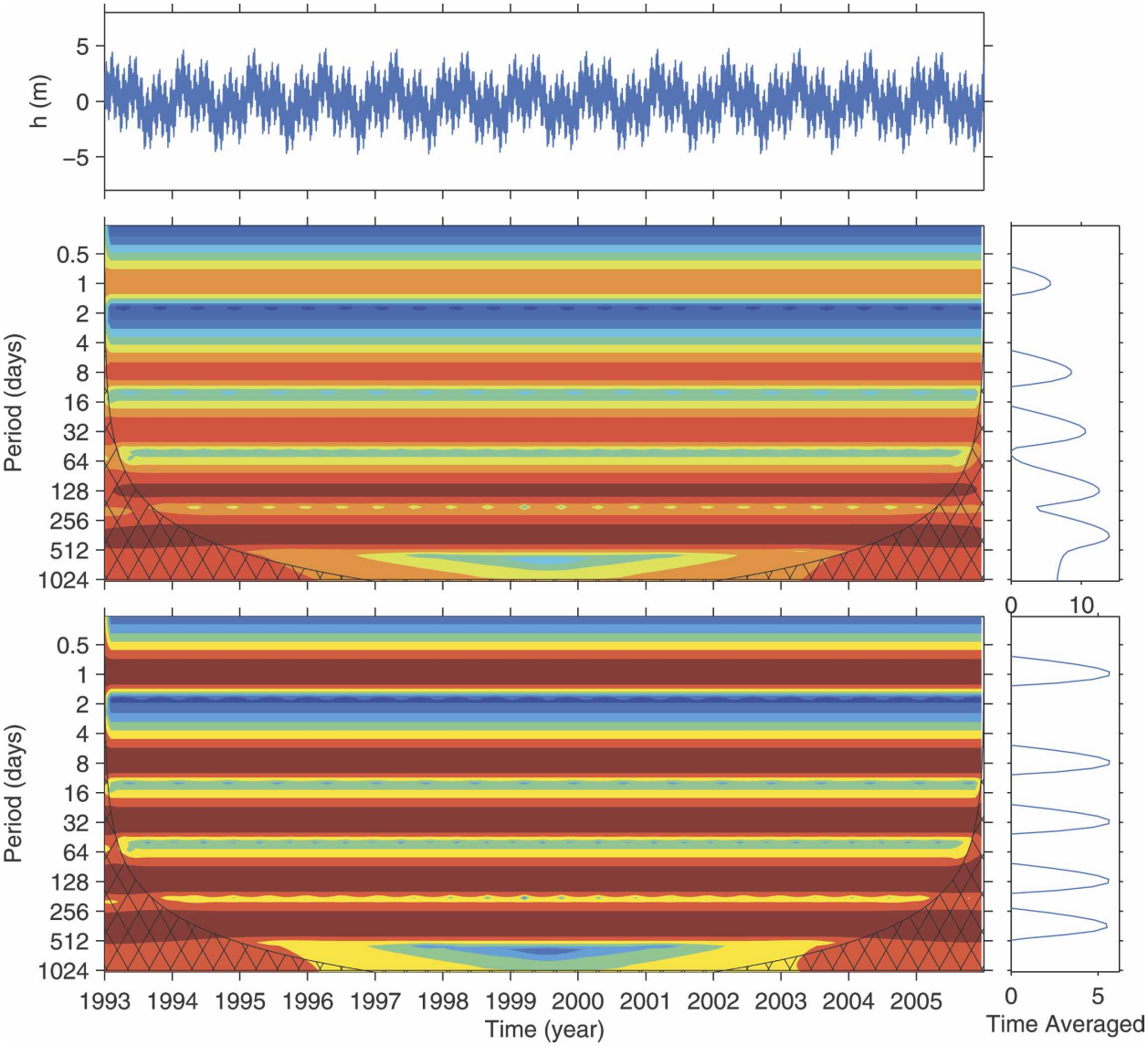

FIG. 2. (top) The artificial time series comprising sine waves of five different periods (1, 8, 32, 128, and 365 days). Also shown are the (middle) original and (bottom) rectified wavelet power spectra (left column) and time-averaged wavelet power spectra (right column) of the artificial time series. Red and blue indicate high and low wavelet power spectrum values (in base 2 logarithm), respectively. Cross-hatched regions indicate the "cone of influence," where edge effects become important.

Fig. 2 (bottom) throughout the time. Thus, both the 128- and 365-day peaks are somehow underestimated.

6. Test with the Niño-3 SST data

It would be illustrative to check some previous wavelet results to see how Eq. (8) may make a difference. A good case study is the wavelet analysis of the Niño-3 SST data, which was given in TC98 as an example of wavelet analysis. This dataset is also well known in both meteorological and oceanographic communities. More detailed information about the dataset can be found in TC98.

The same wavelet parameters are used as those in the MATLAB wavelet package of TC98, that is, Morlet wavelet, starting scale of 6 months, seven powers-of-2 octaves with four suboctaves each. The original and rectified wavelet power spectra are shown in contrast in Fig. 4. Compared to the original wavelet spectrum, there is a slight adjustment of the relative magnitude of the wavelet spectrum across the frequency domain in the rectified spectrum: the high-frequency spectrum

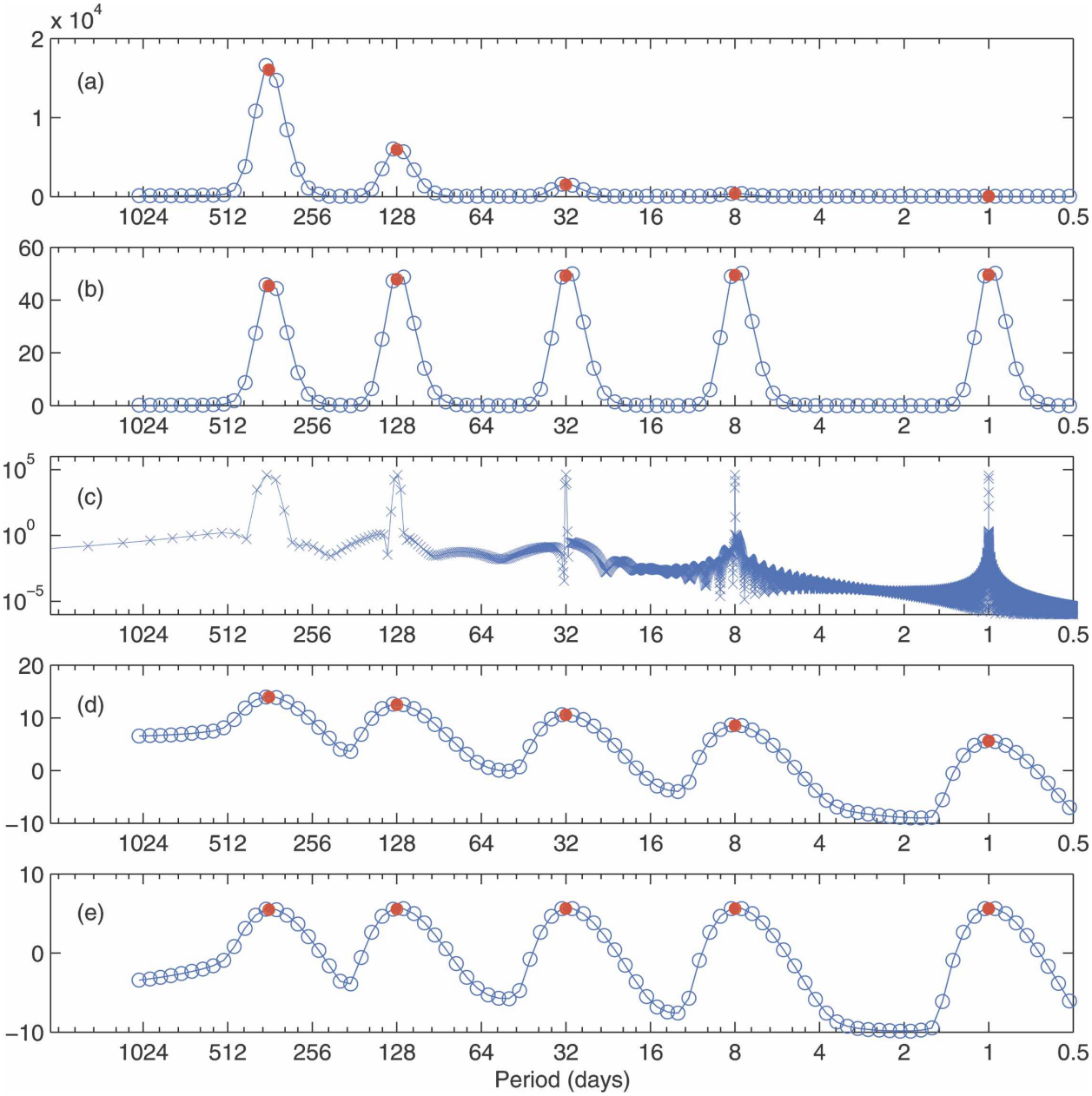

FIG. 3. Power spectra of the artificial sine waves: (a) original time-averaged wavelet power spectrum, (b) rectified time-averaged wavelet power spectrum, (c) Fourier power spectrum; (d), (e) Same as (a) and (b), respectively, except that the wavelet power spectra are shown in base 2 logarithm.

values are decreased, and the low-frequency spectrum values are increased relatively. The adjusted wavelet spectrum overlays better with the 95% significance contours, for example, for the peak area in periods of 3~8 yr during the years 1910~1920. Changes are also found in the time-averaged wavelet spectrum shapes; that is, the spectral line becomes smoother. However, the major peak is still located between the 2- and 8-yr periods. That is, the main conclusion on the Niño-3 SST wavelet analysis in TC98 is not affected.

7. Summary and discussion

The power spectra produced by the wavelet analysis adopted in the mainstream community of the atmosphere–ocean science such as TC98 may be distorted or

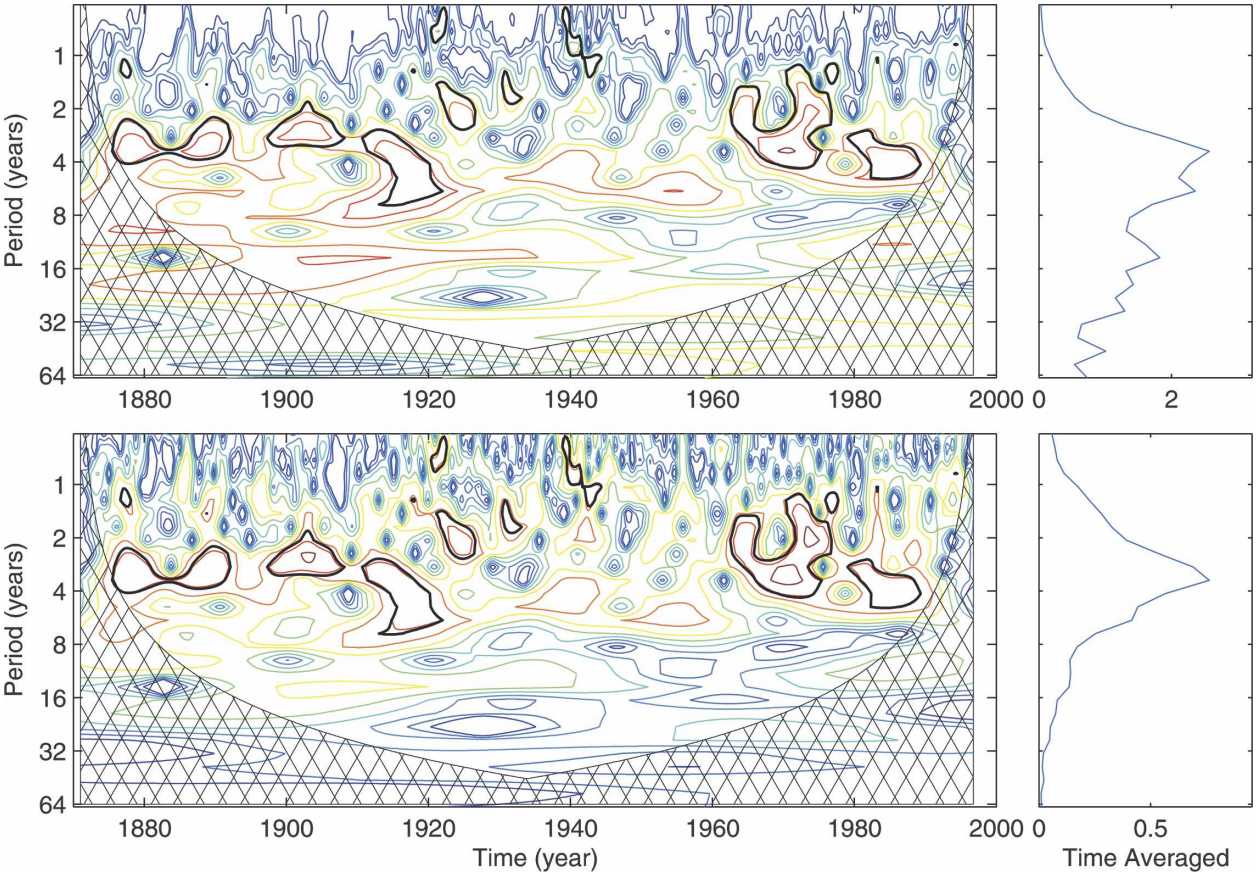

FIG. 4. (top row) Original and (bottom row) rectified wavelet power spectra (left column) and time-averaged wavelet power spectra (right column) from the wavelet analysis of the Niño-3 SST time series. Red and blue contours indicate high and low wavelet power spectrum values, respectively. The regions of greater than 95% confidence are shown with thick black contours. Cross-hatched regions indicate the "cone of influence," where edge effects become important.

biased in favor of large-scale features. Efforts have been made for improvements by TC98 and many others (e.g., Hudgins et al. 1993), but the problem still exists, as revealed in the exercise with the subtidal sea level data of St. Petersburg, Florida, using the software provided by TC98. Unfortunately, this issue was largely overlooked by most wavelet users of the TC98 software package. In TC98, this bias was attributed to the width of the wavelet filter in Fourier space (TC98; also see Torrence and Compo's Web site at http://atoc.colorado.edu/research/wavelets/faq.html). They explained that at small scales (high frequency) the wavelet is very broad in frequency, so any peaks in the spectrum get smoothed out; at large scales, the wavelet is narrower in frequency, so the peaks are sharper and have a larger amplitude. We provided an alternate explanation and a solution to this bias problem.

We established theoretically that the so-called bias actually results from the traditional definition of "energy" for the wavelet power spectra, which has been simply taken as the square of the transform coefficient (to within a constant factor). This is a convention inherited from the Fourier analysis, but unfortunately it is not physically consistent. By the Parseval relation, for analyses with an orthonormal basis, the wavelet transform coefficient squared is equivalent to the integration of the energy (in physical space) at the corresponding instant over the influence period (time scale) the series spans; as a result, a physically consistent definition of energy should be, in an average sense, the transform coefficient squared divided by the scale it associates. By a similar but not rigorous argument, spectra from analyses with other types of bases or redundant frames should also be rectified in such a way to ensure physical consistency. The traditional definition confuses the energy with the energy integrated with respect to time, which will certainly cause a bias in the power spectrum if the integration ranges are different for different scales. This phenomenon stems from the multiresolu-

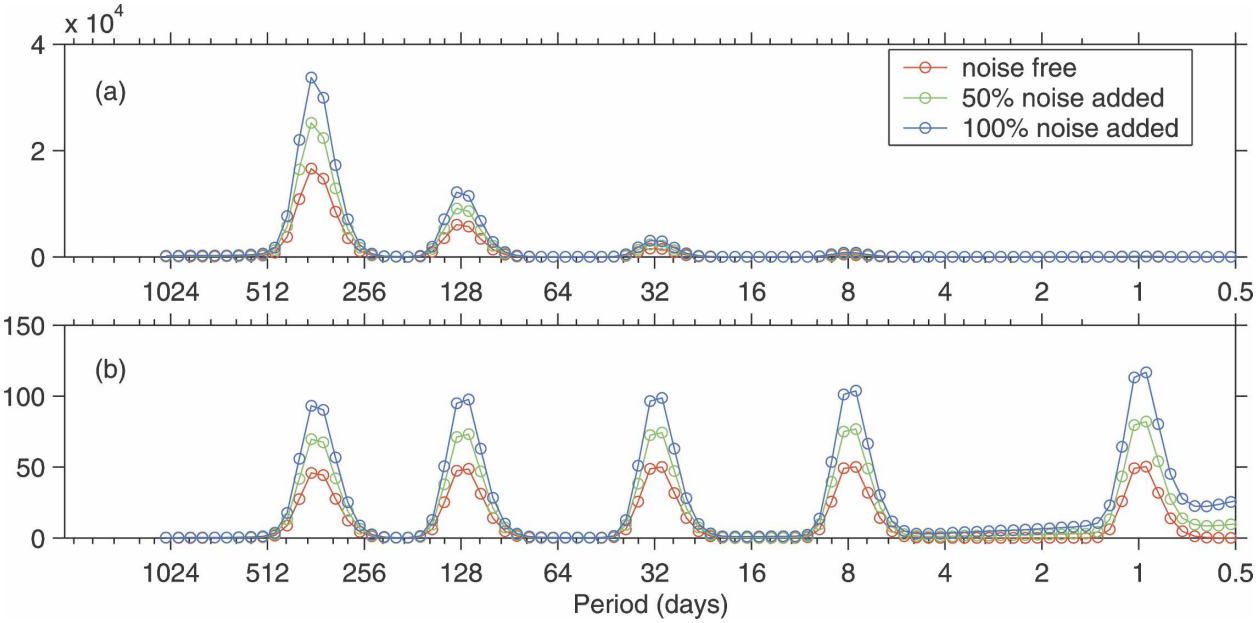

FIG. 5. Time-averaged wavelet power spectra of the artificial sine waves with different noise levels: noise free, and 50% and 100% Gaussian white noise added: (a) original spectra and (b) rectified spectra.

tion analysis, the theoretical foundation of wavelet transform as introduced by Meyer (1992).

The traditional biased power spectra are therefore easily rectified. For that generated by TC98, a simple division of each energy value by the scale it corresponds to will give the correct result. The rectification was applied to the St. Petersburg sea level time series, and the underestimated synoptic weather band energy was brought back to a level comparable with that on annual time scales. The frequency distribution of the rectified wavelet spectrum was more reasonable according to the knowledge of coastal oceanography on the inner WFS. The rectification was also tested with an artificial time series composed of sine waves of known amplitudes and frequencies, and an expected improvement of the biased spectral peaks was obtained. Finally, the classic example of Niño-3 SST in TC98 was reexamined. To our surprise, a similar result is obtained from the original and the rectified spectra. That might be the reason why this issue has been overlooked for so long a time.

It should be pointed out that the definition of energy such as Eq. (8) has appeared in the literature (e.g., Percival 1995; Percival and Mofjeld 1997), though no thorough discussion has been documented from a physical point of view. Unfortunately, this definition has not received enough attention from the meteorology and oceanography community. One possible reason is that the resulting spectrum for Gaussian white noise may no longer be flat across the scales, compared to the flat spectrum using the conventional definition (cf. TC98). We repeated the experiment with Gaussian white noise and found that our spectrum tilted up toward smaller scales (figure not shown). Apparently this is still a problem that deserves further studies. To see how this may affect our previous results, the idealized sine wave experiment in section 5 is repeated by adding Gaussian white noise of 50% and 100% in variance, respectively, and the results are shown in Fig. 5. In the spectra based on definition (8), a small amplification of the peaks and the background spectral values is found in the high-frequency band, while in the low-frequency band the background noise bias is negligible (Fig. 5b). Even for the very noisy data with a signal-to-noise ratio of 1, the five spectral peaks are still clearly seen to have roughly the same height in the rectified spectra, in contrast to those seriously biased in the original spectra.

When connecting wavelet analysis to Fourier analysis, a common practice is to associate scale with frequency. This is a practical convenience but is not entirely true. Given a time series, a scale in the wavelet sense actually contains a range of frequencies. That is to say, if the space where the time series lies is decomposed into a direct sum of a sequence of wavelet subspaces, then each subspace is actually associated with a range of frequencies. These subspaces therefore may be further decomposed. The resulting technique is the well-known wavelet packet transform (e.g., Strang and Nguyen 1997). In a wavelet packet transform, the concept of frequency is more reasonably represented, but the energy definition problem explored in this study

still exists (and becomes more complicated), as underlying the redecomposition is the same machinery, the multiresolution analysis. We will leave that to future studies.

Acknowledgments. Support was by the Office of Naval Research, Grants N00014-05-1-0483 and N00014-02-1-0972. The second of these, for the Southeast Atlantic Coastal Ocean Observing System (SEACOOS), is administered by UNC under Task Order 3-12110-10. Constructive comments were provided by the two anonymous reviewers. Wavelet software was provided by C. Torrence and G. Compo and is available online (see http://paos.colorado.edu/research/wavelets/).

REFERENCES

Chui, C. K., 1992: *An Introduction to Wavelets.* Academic Press, 264 pp.

Cragg, J., G. Mitchum, and W. Sturges, 1983: Wind-induced sea-surface slopes on the West Florida Shelf. *J. Phys. Oceanogr.,* **13,** 2201–2212.

Daubechies, I., 1992: *Ten Lectures on Wavelets*. Society for Industrial and Applied Mathematics, 357 pp.

Domingues, M. O., O. Mendes, and A. M. da Costa, 2005: On wavelet techniques in atmospheric sciences. *Adv. Space Res.,* **35,** 831–842.

Gamage, N., and W. Blumen, 1993: Comparative analysis of low-level cold fronts: Wavelet, Fourier, and empirical orthogonal function decompositions. *Mon. Wea. Rev.,* **121,** 2867–2878.

Gu, D., and S. G. H. Philander, 1995: Secular changes of annual and interannual variability in the Tropics during the past century. *J. Climate,* **8,** 865–876.

Haus, B. K., and H. C. Graber, 2000: Analysis of non-stationary vector fields using wavelet transforms. *Proc. Oceans 2000 MTS/IEEE Conf.*, Vol. 3, Providence, RI, MTS/IEEE, 1521–1527.

——, ——, and L. K. Shay, 1999: Wavelet analysis of surface current vector fields measured by High Frequency Doppler radar. *Proc. IEEE Sixth Working Conf. on Current Measurement,* San Diego, CA, IEEE, 19–24.

He, R., Y. Liu, and R. H. Weisberg, 2004: Coastal ocean wind fields gauged against the performance of an ocean circulation model. *Geophys. Res. Lett.,* **31,** L14303, doi:10.1029/2003GL019261.

Hudgins, L., C. A. Friehe, and M. E. Mayer, 1993: Wavelet transforms and atmospheric turbulence. *Phys. Rev. Lett.,* **71,** 3279–3282.

Labat, D., 2005: Recent advances in wavelet analyses: Part 1. A review of concepts. *J. Hydrol.,* **314,** 275–288.

Lau, K.-M., and H.-Y. Weng, 1995: Climate signal detection using wavelet transform: How to make a time series sing. *Bull. Amer. Meteor. Soc.,* **76,** 2391–2402.

Li, Z., and R. H. Weisberg, 1999: West Florida continental shelf response to upwelling favorable wind forcing, 2. Dynamics. *J. Geophys. Res.,* **104,** 23 427–23 442.

Liang, X. S., and A. R. Robinson, 2004: A study of the Iceland-Faeroe frontal variability with the multiscale energy and vorticity analysis. *J. Phys. Oceanogr.,* **34,** 2571–2591.

——, and ——, 2005: Localized multiscale energy and vorticity analysis, I. Fundamentals. *Dyn. Atmos. Oceans,* **38,** 195–230.

——, and D. G. M. Anderson, 2007: Multiscale window transform. *SIAM J. Multiscale Model. Simul.,* **6,** 437–467.

Liu, P. C., 1994: Wavelet spectrum analysis and ocean wind waves. *Wavelets in Geophysics,* E. Foufoula-Georgiou and P. Kumar, Eds., Academic Press, 151–166.

——, and G. S. Miller, 1996: Wavelet transforms and ocean current data analysis. *J. Atmos. Oceanic Technol.,* **13,** 1090–1099.

Liu, Y., and R. H. Weisberg, 2005a: Momentum balance diagnoses for the West Florida Shelf. *Cont. Shelf Res.,* **25,** 2054–2074.

——, and ——, 2005b: Patterns of ocean current variability on the West Florida Shelf using the self-organizing map. *J. Geophys. Res.,* **110,** C06003, doi:10.1029/2004JC002786.

——, and ——, 2007: Ocean current structures and sea surface heights estimated across the West Florida Shelf. *J. Phys. Oceanogr.,* **37,** 1697–1713.

——, ——, and L. K. Shay, 2007: Current patterns on the West Florida Shelf from joint Self-Organizing Map analyses of HF radar and ADCP data. *J. Atmos. Oceanic Technol.,* **24,** 702–712.

Marmorino, G. O., 1982: Wind-forced sea level variability along the West Florida Shelf (winter, 1978). *J. Phys. Oceanogr.,* **12,** 389–405.

Meyer, Y., 1992: *Wavelets and Operators*. Cambridge University Press, 223 pp.

Meyers, S. D., B. G. Kelly, and J. J. O'Brien, 1993: An introduction to wavelet analysis in oceanography and meteorology: With application to the dispersion of Yanai waves. *Mon. Wea. Rev.,* **121,** 2858–2866.

Mitchum, G. T., and W. Sturges, 1982: Wind-driven currents on the West Florida Shelf. *J. Phys. Oceanogr.,* **12,** 1310–1317.

Pawlowicz, R., B. Beardsley, and S. Lentz, 2002: Classical tidal harmonic analysis including error estimates in MATLAB using T-TIDE. *Comput. Geosci.,* **28,** 929–937.

Percival, D. B., 1995: On estimation of the wavelet variance. *Biometrika,* **82,** 201–214.

——, and H. O. Mofjeld, 1997: Analysis of subtidal coastal sea level fluctuations using wavelets. *J. Amer. Stat. Assoc.,* **92,** 868–880.

——, and A. T. Walden, 2000: *Wavelet Methods for Time Series Analysis.* Cambridge University Press, 594 pp.

Strang, G., and T. Nguyen, 1997: *Wavelets and Filter Banks*. Revised ed. Wellesley-Cambridge Press, 520 pp.

Torrence, C., and G. P. Compo, 1998: A practical guide to wavelet analysis. *Bull. Amer. Meteor. Soc.,* **79,** 61–78.

Wang, B., and Y. Wang, 1996: Temporal structure of the Southern Oscillation as revealed by waveform and wavelet analysis. *J. Climate,* **9,** 1586–1598.

Weisberg, R. H., and R. He, 2003: Local and deep-ocean forcing contributions to anomalous water properties on the West Florida Shelf. *J. Geophys. Res.,* **108,** 3184, doi:10.1029/2002JC001407.

——, ——, Y. Liu, and J. Virmani, 2005: West Florida Shelf circulation on synoptic, seasonal, and interannual time scales. *Circulation in the Gulf of Mexico: Observations and Models, Geophys. Monogr.,* Vol. 161, Amer. Geophys. Union, 325–347.

Willemsen, J. E., 1995: Analysis of SWADE Discus N wind speed and wave height time series. Part I: Discrete wavelet packet representations. *J. Atmos. Oceanic Technol.,* **12,** 1248–1270.